



Published in final edited form as:

*J Neurosci Methods*. 2008 May 15; 170(1): 1–8. doi:10.1016/j.jneumeth.2007.12.008.

## Efficient Estimation of Retinal Ganglion Cell Number: a Stereological Approach

**John B. Fileta, Wei Huang, Gina P. Kwon, Theodoros Filippopoulos, Yixin Ben, Adam Dobberfuhr, and Cynthia L. Grosskreutz**

Howe Laboratory of Ophthalmology, Massachusetts Eye and Ear Infirmary, Harvard Medical School, 243 Charles Street, Boston, MA 02114, USA

### Abstract

Retinal ganglion cells (RGCs) are the only output neurons of the retina, and their degeneration after damage to the optic nerve or in glaucoma is a well established system for studying apoptosis in the central nervous system. Frequently used procedures for assessing RGC number in retinal flat mounts suffer from two problems: RGC densities are not uniform across retinal flat mounts, and density measures may therefore not reflect total number, and flat mounts do not allow efficient use of tissue. To overcome these problems we developed a stereological method for efficiently assessing RGC number in cryostat sections of the retina. We empirically demonstrate that only ~1:20 sections need be assessed to accurately estimate the total number of RGCs in the rat retina, providing ample tissue for additional studies in the same retina and saving considerably on more exhaustive sampling strategies. Using this method, we estimate that there are  $86,282 \pm 4,759$  RGCs in the normal Brown-Norway rat retina. These counts match well with estimates of axon counts in optic nerve. In a pilot study of experimental glaucoma, we determined a reduction of RGCs to  $53,862 \pm 4272$  ( $p < 0.05$ ). The current technique should prove advantageous to assess neuroprotective strategies in these experimental models.

### Keywords

retinal ganglion cells; stereology; glaucoma; optic nerve; retina

### Introduction

Retinal ganglion cells (RGCs) are the sole projection relaying visual information from the eye to the brain by way of their axons in the optic nerve, and when these cells die, portions of the retina can no longer send visual signals to the brain. RGCs have been shown to die by apoptosis in various models of cell death such as optic nerve crush (Berkelaar et al., 1994), optic nerve axotomy (Isenmann et al., 1997), ischemia (Selles-Navarro et al., 1996; Guo et al., 2003), anterior ischemic optic neuropathy (Bernstein et al., 2007) and glaucoma (Quigley, 1999; Huang et al., 2005a; Hanninen et al., 2002). Quantification of RGC numbers is essential for

---

Please address correspondence to: Cynthia L. Grosskreutz. MD PhD, Howe Laboratory of Ophthalmology, Massachusetts Eye and Ear Infirmary, Harvard Medical School, 243 Charles Street, Boston, MA 02114, USA. Phone 617 573 4328, FAX, Email [cynthia\\_grosskreutz@meei.harvard.edu](mailto:cynthia_grosskreutz@meei.harvard.edu).

**Publisher's Disclaimer:** This is a PDF file of an unedited manuscript that has been accepted for publication. As a service to our customers we are providing this early version of the manuscript. The manuscript will undergo copyediting, typesetting, and review of the resulting proof before it is published in its final citable form. Please note that during the production process errors may be discovered which could affect the content, and all legal disclaimers that apply to the journal pertain.

assessing pathologic damage, pharmacological effects and protection, and a better understanding of disease mechanisms in the eye and optic nerve.

Accurate quantification of *in vivo* studies requires clear and unambiguous identification of cell types within the retina. The fluorescent tracer Fluorogold has been established as an excellent marker of RGCs. When Fluorogold is injected into the superior colliculi of the brain, RGCs take up the dye by retrograde axonal transport (Selles-Navarro et al., 1996). Over 90% of rat RGCs can be labeled by injection into the superior colliculus (Linden and Perry, 1983).

Previous methods of RGC quantification and damage assessment have used calculations based on RGC density (Fukuda, 1977; Hou et al., 2004), optic nerve axon counts (Levkovitch-Verbin et al., 2002; Chauhan et al., 2002; Cepurna et al., 2005), automated flatmount counts (Danias et al., 2002; Danias et al., 2006), and fluorescent whole mount counting methods (Schlamp et al., 2001; Maeda et al., 2004; Park et al., 2001). We and others have previously applied stereological counts to retinal whole mounts, but these procedures are time consuming and require a significant investment of tissue and effort for a single counting output (Freeman and Grosskreutz, 2000; Hanninen et al., 2002; Bernstein et al., 2007). A major consideration in RGC quantification is the requirement of an entire retina for processing, effectively limiting the use of any retinal tissue for further studies. We have adapted the method of stereological counting to retinal cross-sections to enable the combination with other analyses performed in retinal tissue sections such as immunohistochemistry, laser capture microdissection, and qPCR. This provides a powerful method whereby RGC counts can be correlated with specific biological readouts.

In the retina, there is a considerable degree of variability in RGC density, which makes estimates based on density alone difficult and susceptible to significant variations due to artificial swelling or shrinkage as a result of tissue preparation or disease processes. Stereology is an efficient, repeatable, and accurate counting method that overcomes some of these difficulties and intrinsic biases.

Stereology is a systematic and statistically unbiased counting method that does not depend on tissue size, shape, or distribution. It has been widely applied in neuropathological and anatomical studies for quantifying such things as the number of axons in nerve cross sections (Larsen, 1998), neurite outgrowth (Ronn et al., 2000), synapses in various brain regions (Geinisman et al., 1996), and neuronal loss (Gomez-Isla et al., 1997; Hyman et al., 1998; West et al., 2004); for review see (Gundersen et al., 1988; Schmitz and Hof, 2005). In this study we have adapted the technique of unbiased stereological counting to estimate the total number of RGCs per retina in retinal cross-sections, and apply the technique to quantifying RGC death in experimental glaucoma.

## Materials and Methods

### Animals

Adult male Brown Norway rats (300–450 g, Charles River, Boston, MA) were used in these studies. Animals were housed in covered cages and were fed with a standard rodent diet *ad libitum*, while kept on a 12h light – 12h dark cycle. All procedures concerning animals were in accordance with the statement of The Association for Research in Vision and Ophthalmology for the use of animals in research.

### Backlabeling of Retinal Ganglion Cells

Anesthesia was induced using a mixture of acepromazine maleate (1.5 mg/kg), xylazine (7.5 mg/kg), and ketamine (75 mg/kg) (all from Webster Veterinary Supply, Sterling, MA). Deeply anesthetized rats were placed in a stereotaxic apparatus (Kopf Instruments, Tujunga, CA) and

the skin overlying the skull was cut open and retracted. The skull was leveled using the lambda and bregma sutures as landmarks. A burr attached to a dremel tool (Dremel, Robert Bosch Tool Corporation, Mount Prospect, IL) was used to thin the skull and an injector was lowered into the superior colliculus 5.3 mm posterior to bregma, 1.5 mm lateral to midline, and 4.8 mm ventral to the skull surface. Two  $\mu$ l of a 3% Fluorogold (Fluorochrome LLC., Denver, CO) solution in PBS with 10% DMSO was then injected slowly over 10 minutes. The procedure was repeated on the contralateral side of the brain, the skin closed with a 4-0 silk suture, antibiotic ointment applied to the wound, and the animal allowed to recover from anesthesia in its home cage (Huang et al., 2005a). To ensure adequate backlabeling of RGCs, animals were allowed seven days for retrograde transport of Fluorogold before further experimental interventions (including induction of glaucoma). This backlabeling technique is effective for RGCs with normal transport, as would be expected prior to the induction of glaucoma.

### Tissue preparation

For RGC counting, animals were sacrificed by CO<sub>2</sub> inhalation and subjected to intracardiac perfusion with PBS followed by 4% paraformaldehyde (PFA) in PBS. After perfusion, the eyes were postfixed in 4% PFA for 1h and cryoprotected with serial sucrose dilutions. Eye cups were frozen in optimal cutting temperature compound (OCT) (Tissue-Tek®, Miles Diagnostic Division, Elkhart, IN) and sectioned in their entirety at 16 $\mu$ m. Approximately 450 sections/eye were mounted on Superfrost Plus slides (VWR company, West Chester, PA), and stored at -80°C. Tissue sections were incubated in a blocking solution of 1% bovine serum albumin for 1 h at room temperature, and then incubated overnight at 4°C with a primary antibody specific for Fluorogold (1:200 Fluorochrome LLC., Denver, CO). The sections were rinsed three times in PBS, incubated with secondary antibody (goat biotinylated anti-rabbit IgG (1:500, Vector Laboratories, Burlingame, CA)) for 1 hour at room temperature, rinsed three times in PBS, and incubated in avidin-biotin-peroxidase complex (Vector Laboratories, Burlingame, CA) in PBS for 30 min at room temperature. Coloration was performed in double distilled H<sub>2</sub>O containing diaminobenzidine (DAB) and hydrogen peroxide. Methyl Green (Vector Laboratories) was used to counterstain the nuclei.

Optic nerves were obtained from three control eyes, preserved in glutaraldehyde, embedded in EPON and semithin (1 micrometer) sections obtained and stained with toluidine blue.

### Stereological Quantification of RGCs

**Equipment**—All stereological analysis was carried out by manually counting Fluorogold positive cells using the Olympus C.A.S.T. System (Version 2.3.1.2; Olympus, Albertslund, Denmark) composed of an Olympus BX51 microscope connected to an Olympus DP70 digital camera and a computer controlled X-Y-Z step motor stage ProScan (PRIOR Scientific, Rockland, MA).

**Sampling Principles**—Unbiased stereological sampling is based on the principle that any RGC has an equal probability of being sampled independent of its location, size, and shape. It is unbiased in that the larger the sampling group, the more closely you approach the actual value (Gundersen et al., 1988). By sampling select portions of the entire retina, we are able to create an informed, accurate, and high reproducible estimate of the total RGC number. This smaller sample pool must be *representative*, i.e. randomly selected and must be from a group composed of the region of interest, in this case the *entire* retina. This sampling technique allows a smaller, more manageable and tissue sparing sample group that accurately represents the total retina.

The area of interest (the RGC layer) was delineated on the Olympus C.A.S.T. System and a counting frame (see below for detail) was randomly placed within the RGC layer to mark the

first area to be sampled. Systematic samples are then chosen over a defined and uniform interval through the entire delineated RGC layer as shown in Figure 1.

**Counting Principles**—The optical fractionator (Gundersen, 1986; West et al., 1991), the optical dissector (Bjugg and Gundersen, 1993) and the counting frame provide the rules for what profiles should be counted within the delineated counting area (Fig. 2). The fractionator refers to a sampling scheme in which a predetermined number of sections over a uniform interval are selected from a known fraction. The optical dissector is a three-dimensional probe for direct counting of objects in a defined volume. Application of the counting frame (Figure 2), fractionator sampling scheme, and optical dissector are illustrated (Figure 3).

Random, systematic, and uniform sampling, through the retina in which the optical dissector is applied ensures that all RGCs have an equal possibility of being sampled, that all samples are randomly selected regardless of morphology, and that all counted samples are counted only once, preventing overestimation. RGCs were identified by Fluorogold backlabeling (immunostained and visualized with DAB), morphology and position in the retinal ganglion cell layer. DAB positive RGCs were further identified when the DAB reaction product was present in a cellular distribution (i.e. cell body, excluded from the nucleus, processes) and at a level above the overall background staining in the inner nuclear layer.

In this study the first retinal section to be counted is chosen by using a random number generator (for a number between 1 and 10) and represents a known fraction of the entire retina. Following delineation of the region of interest, the RGC layer (Figure 1), every  $N^{\text{th}}$  section thereafter is sampled and counted, dependent on sampling intensity. In each sampled section RGCs are directly counted using optical dissectors (Figure 3) in a uniform grid of x, y positions. The counting frame (Fig 2) is placed at an initially random, then uniformly translated in steps (x,y) over each grid by the motorized microscope stage, systematically sampling throughout the entire section. Individual RGCs are directly counted when they lie within the area of the counting frame and meet the optical dissector counting rules as the focal plane is moved through the thickness of the section (Figure 3). Guard zones of 3  $\mu\text{m}$  at the top and bottom of the Z planes were utilized so that the counts were obtained in the central 10  $\mu\text{m}$  of the tissue section. Subsequent sections were selected systematically following a constant sampling intensity of every  $N^{\text{th}}$  section. In normal eyes, 5% of the region of interest (the RGC layer) on every  $N^{\text{th}}$  ( $N=6, 12, 18, 24, 30, 36, 42, 48$ ) section was counted. Since we expected at least a 30% loss of RGCs in the glaucoma eyes, we counted 10% of the region of interest (the RGC layer) of every  $N^{\text{th}}$  section (as opposed to 5% in normal eyes) in order to count approximately the same number of RGCs in normal and glaucomatous eyes. RGCs were directly counted through a known fraction of the delineated retina.

These sampling intensities were adopted to determine an acceptable coefficient of error (CE) (Glaser and Wilson, 1998) and coefficient of variation (CV) (Tandrup, 2004) calculated for both control and experimental eyes and computed from:

$$CE=1/\sqrt{Q} \quad \text{Equation 1}$$

$$CV(\text{Obs})^2=CV(\text{Biol})^2+CE^2 \quad \text{Equation 2}$$

where Q is equal to the number of profiles counted within sampled fractions,  $CV(\text{Obs}) = SD/\text{Mean}$ , and  $CV(\text{Biol})$  is biological variation. The coefficient of error is an expression of the precision of an estimate, while the coefficient of variation is a relative measure of variation

compared to the mean. For stereological sampling to be efficient the CE must be smaller than biological variation (~10%).

**Number Estimation**—The total number (N) of RGCs in the retina was estimated based on the stereological algorithm (West et al., 1991):

$$N = \sum Q \cdot 1/sf \cdot tf/sf \quad \text{Equation 3}$$

Where  $\sum Q$  is the total number of RGCs counted within the dissector of sampled fractions,  $tf$  is the total number of fractions contained in the totally sectioned eye, and  $sf$  is the number of sampled fractions. Approximately 18–24 sample fractions were necessary to sample the retina in its entirety. Total axon number was estimated in normal optic nerves using the fractionator approach, counting axons in approximately twenty,  $100 \mu\text{m}^2$  counting frames for each optic nerve.

### Experimentally-induced glaucoma

Unilateral elevation of IOP was produced by injecting hypertonic saline into aqueous veins of Brown Norway rats, as previously described by Morrison (Morrison et al., 1997). Briefly, hypertonic 1.9 M saline was injected into limbal aqueous humor collecting veins of the left eye. The right eye served as a control. In cases where the IOP was not elevated within 2 weeks, re-injection was performed in a different episcleral vein. A maximum of 3 injections were performed.

### Intraocular pressure (IOP) determination

All IOP measurements in rats were performed with animals in the awake state between 10am and 2pm to minimize diurnal variability in IOP. After applying a drop of 0.5% proparacaine local anesthesia, IOP was measured using a TonoPen XL tonometer (Medtronic Ophthalmics, Jacksonville, FL) (Moore et al., 1993). Fifteen readings were taken for each eye and averaged. Baseline IOP was obtained on three consecutive days before the first saline injection, and three times per week thereafter. Animals were subjected to a 10 day period of elevated IOP exposure. IOP was considered elevated if the IOP was consistently greater than 35 mmHg at consecutive determinations. After IOP had been elevated for 10 days, rats were killed with  $\text{CO}_2$  asphyxiation, and the eye-cups were collected for analysis. As an estimate of IOP exposure we integrated IOP with time, which takes into account both the length and the degree of IOP exposure. Integrated IOP was calculated as the area under the pressure - time curve (experimental eye - control eye), beginning with the day of the 1<sup>st</sup> saline injection. Animals were included in the analysis only if they had peak IOP > 40 mmHg and integrated IOP > 280 mmHg-days. The threshold of 200 mmHg-days has been reported to be the point at which RGC loss begins and after which RGC loss progresses rapidly (McKinnon, 2003). All animals meeting these criteria were included in the analysis. Animals not meeting these criteria were not evaluated.

### Statistical analysis

NCSS (NCSS Statistical Software, Kaysville, Utah) was used to perform all statistical analyses. Results are expressed as mean  $\pm$  standard deviation. Paired comparisons were performed using a Student's t-test and significance assessed at the 0.05 level.

## Results

### Sampling Intensity

A normal eye was used to determine the effect of sampling intensity on RGC estimation. Predetermined periodicity between sampled sections ( $N^{\text{th}}$  section counted) counted,  $\Sigma Q$ , CE, CV, and total RGCs estimates are reported in Table 2. All sampling intensities were within acceptable CE limits (10%), although estimates based on sampling intensities with CE values  $\leq 8\%$  (trials 1–4) demonstrate remarkable precision and accuracy. 5% of each retinal section was counted, but the total number of sections counted varied from 7 to 41 retinal cross-sections. By increasing sample size from 7 to 41 retinal cross-sections there is only a modest improvement in estimate accuracy. Even an increase of nearly four fold in sampling intensity (trial 4 of 11 sections to trial 1 of 41 sections) does not significantly improve RGC estimates, but does considerably increase tissue preparation and counting time proportionally.

### RGC estimates of Normal Eyes in Brown Norway Rats

The stereological estimates for the total number of Fluorogold positive RGCs in a normal Brown Norway rat eye are shown in Table 1, in addition to CE, CV, and  $\Sigma Q$  values associated with RGC total estimates for 10 animals. 5% of the region of interest (the RGC layer) of every 18<sup>th</sup> retinal cross section was counted, a mean of 221 RGCs were counted per eye for total RGC estimates. RGC counts ranged from 79,748 to 93,422 cells with a mean ( $\pm$  s.d.) of  $86,282 \pm 4,759$ . This range of RGC counts demonstrates that the inter-animal variability is larger than the variability introduced by stereological estimation. Therefore, the power of the counting analysis will be improved by counting more animals rather than by counting more slides per animal.

To provide an independent assessment of the accuracy of the RGC counts we performed stereological counting on retinal flat mounts and also prepared semi-thin sections of optic nerve and carried out stereologic axon counts on three normal eyes (estimates from  $\sim 20, 100 \mu\text{m}^2$  fields). These estimates were  $80,728 \pm 3913$  ( $n=8$ ) for flat mounts and averaged 92,068 axons ( $n=3$ ) ranging from 82,044 to 102,900 ( $sd = 10,707$ ), comparing well with RGC estimates (mean 86,282), considering that one would expect 5,000 – 10,000 more axons than RGCs backlabeled from the superior colliculus.

### Elevation of IOP

IOP was surgically elevated in one eye of each rat with the fellow eye serving as a control. After 10 days, animals had a mean of  $18.1 \pm 0.9$  mmHg in control eyes and a mean of  $43.3 \pm 1.4$  mmHg in elevated IOP eyes. For inclusion in this study animals had to have a mean IOP  $> 40$  mmHg and an integrated IOP  $> 280$  mmHg-days. These strict criteria were used to minimize the variability introduced by IOP differences. Rats were killed after 10 days of elevated IOP.

### RGC loss in Experimental Glaucoma

RGC counts, CE, CV, and percentage of cell loss per animal as a result of experimental glaucoma are reported in Table 3. RGC counts in control eyes ranged from 78,000 to 93,600 with a mean ( $\pm$ s.d.) of  $84,862 \pm 5,753$ , as previously reported for some eyes (Huang et al., 2005a; Huang et al., 2005b). In eyes with elevated IOP for 10 days RGC counts ranged from 51,100 to 63,029 with a mean of  $56,837 \pm 4,272$ , indicating a 33% loss of RGCs ( $n=8$ ;  $p < 0.05$ ).



## Discussion

Quantification of RGC number in normal and diseased states of animal models is essential to better understanding mechanisms of RGC apoptosis and potential pathways for neuroprotection and regeneration. The present study describes an adaptation of the method of stereology for efficient, systematic, and precise RGC counting in retinal cross-sections, thereby allowing both accurate quantitation of RGC number and considerable experimental flexibility compared to whole mount preparations. Applying established Fluorogold backlabeling techniques and stereological counting methods, a small number of retinal cross-sections can be used to create accurate estimates of entire RGC populations.

Our lab has previously applied stereology to retinal whole mounts to estimate the total number of RGCs in Brown Norway rats and estimate a mean of  $74,104 \pm 4,166$  ( $\pm$  SEM) RGCs (Freeman and Grosskreutz, 2000) which correlates well with our current estimates of  $80,728 \pm 3913$  for whole mounts. Danias et al. have recently reported RGC estimates using automated counts of retinal whole mounts with a range of 57,978 to 88,131 (mean of 73,490) RGCs (Danias et al., 2006). Although slightly lower, both estimates are well correlated with our current result of a range of 79,748 to 93,422 RGCs (mean of 86,282) estimated by cross-sectional stereological counting. The latter counts also correlate well with our own estimates of axon number in the optic nerve (mean 92,068).

Due to tissue thickness, weakly backlabelled RGCs may not be easily detected in whole mounts, whereas the immunostaining protocol for Fluorogold employed in cryostat sections likely enhances sensitivity of the technique. Use of the optical dissector, in which cells are rejected if present at the top of the counting chamber (initial optical plane) guards against double counting of split neurons in the cryostat sections. These estimates of RGC and axon number are lower than the mean count of 117,900 obtained by optic nerve axonal counts (Cepurna et al., 2005). This variance may be due to multiple factors including age of the animals, projection of a small percentage of RGCs to the lateral geniculate nucleus, a small percentage of recurrent or branched axons, or strain and biological variability, as noted below.

When assessing RGC counts and cell loss of *in vivo* disease models, an important consideration is the genetic difference and resulting variation of RGC numbers between strains. In mice, a comparison between 38 recombinant strains revealed a large natural variation, more than 20,000 RGCs (range of 51,000 to 75,000), between various strains of mice (Williams et al., 1998). Between Brown Norway and Wistar rats there is a 24,000 difference in total mean RGC counts (Wistar mean 97,609 and Brown Norway mean 73,490) (Danias et al., 2002; Danias et al., 2006). Such large variance between strains brings to light the importance of efficient, accurate, and reproducible counting methods for precise estimations of RGCs, and use, whenever possible, of within animal or littermate controls.

Biological variation and RGC estimation are important considerations when one performs a power analysis and is determining sample size. The more accurate and reliable a counting method, the smaller the sample group needed to detect statistically significant differences. Cross-sectional stereological counting produces highly accurate and reproducible counts. Standard deviations were less than 7% of total RGCs mean in all animals, comparable to previous RGC estimates by axonal count (9%) (Cepurna et al., 2005) and whole mount counts (12%) (Danias et al., 2006).

In addition to providing an efficient method of accurately assessing RGC number, the technique is advantageous because remaining cross-sections not used in estimating RGC numbers are available for any number of molecular and histological studies. In addition to the savings involved in not having to prepare additional animals for such studies, importantly, all collected data can be directly correlated with RGC counts from the exact eye. For example, we have

previously coupled cross-sectional stereological counting with laser capture microdissection (LCM) and qPCR analysis to demonstrate an upregulation of Caspase 8 and 9 mRNA in experimental glaucoma (Huang et al., 2005a). We also applied the method of cross-sectional stereological counting as a tool for assessing RGC survival and neuroprotection in experimental glaucoma as a result of drug treatment. In glaucoma eyes treated with the calcineurin inhibitor FK506, stereological counting methods detected a 50% protection of RGCs (Huang et al., 2005b).

Stereology principles, including the use of systematic random sampling in which each part of the total volume of tissue has an equal chance of being counted, often allows accurate estimation of total number even when only a relatively small fraction of the total volume is counted. Our data (Table 1) show, for example, that the count estimates do not further improve even when sampling fraction is increased 4 fold from 4% (1 in 24) to 16% (1 in 6). Moreover, the counting rules preclude double counting from split cells and overcome potential bias introduced by differences in cell size, shape or orientation.

Previous techniques for quantifying RGC numbers and changes in experimental models were time consuming, potentially intrinsically biased, and required large tissue investments. By applying the technique of unbiased stereological counting, retinal cross-sections can be used for RGC estimation. Thus the technique of stereological counting in retinal cross-sections provides a powerful, efficient, and accurate tool with which to estimate the total number of RGCs per retina and preserve tissue for further analysis.

## Acknowledgments

This work was supported by National Institutes of Health Grant R01EY13399, a Research to Prevent Blindness Career Development Award (New York), and the Massachusetts Lions Eye Research Fund. We gratefully acknowledge Bradley T. Hyman, M.D., Ph.D. and Matthew Frosch, M.D., Ph.D. (Departments of Neurology and Neuropathology, Mass General Institute for Neurodegenerative Disease, Massachusetts General Hospital, Boston, MA), for helpful comments and suggestions and Kellen J. Scott for artistic help.

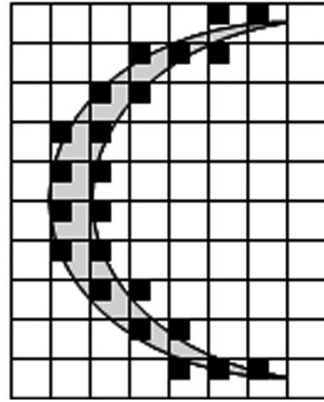
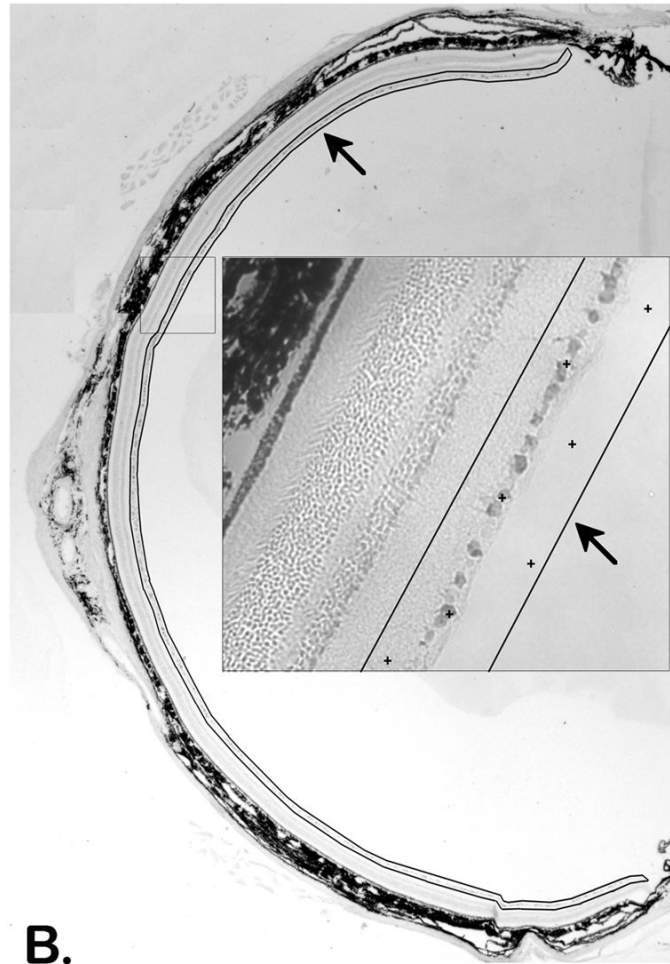
## References

- Berkelaar M, Clarke DB, Wang YC, Bray GM, Aguayo AJ. Axotomy results in delayed death and apoptosis of retinal ganglion cells in adult rats. *J Neurosci* 1994;14:4368–74. [PubMed: 8027784]
- Bernstein SL, Guo Y, Slater BJ, Puche A, Kelman SE. Neuron stress and loss following rodent anterior ischemic optic neuropathy in double-reporter transgenic mice. *Invest Ophthalmol Vis Sci* 2007;48:2304–10. [PubMed: 17460295]
- Bjugn R, Gundersen HJ. Estimate of the total number of neurons and glial and endothelial cells in the rat spinal cord by means of the optical disector. *J Comp Neurol* 1993;328:406–14. [PubMed: 8440788]
- Cepurna WO, Kayton RJ, Johnson EC, Morrison JC. Age related optic nerve axonal loss in adult Brown Norway rats. *Exp Eye Res* 2005;80:877–84. [PubMed: 15939045]
- Chauhan BC, Pan J, Archibald ML, LeVatte TL, Kelly ME, Tremblay F. Effect of intraocular pressure on optic disc topography, electroretinography, and axonal loss in a chronic pressure-induced rat model of optic nerve damage. *Invest Ophthalmol Vis Sci* 2002;43:2969–76. [PubMed: 12202517]
- Danias J, Shen F, Goldblum D, Chen B, Ramos-Esteban J, Podos SM, Mittag T. Cytoarchitecture of the retinal ganglion cells in the rat. *Invest Ophthalmol Vis Sci* 2002;43:587–94. [PubMed: 11867571]
- Danias J, Shen F, Kavalarakis M, Chen B, Goldblum D, Lee K, Zamora MF, Su Y, Brodie SE, Podos SM, Mittag T. Characterization of retinal damage in the episcleral vein cauterization rat glaucoma model. *Exp Eye Res* 2006;82:219–28. [PubMed: 16109406]
- Freeman EE, Grosskreutz CL. The effects of FK506 on retinal ganglion cells after optic nerve crush. *Invest Ophthalmol Vis Sci* 2000;41:1111–5. [PubMed: 10752948]
- Fukuda Y. A three-group classification of rat retinal ganglion cells: histological and physiological studies. *Brain Res* 1977;119:327–34. [PubMed: 830390]



- Geinisman Y, Gundersen HJ, van der Zee E, West MJ. Unbiased stereological estimation of the total number of synapses in a brain region. *J Neurocytol* 1996;25:805–19. [PubMed: 9023726]
- Glaser EM, Wilson PD. The coefficient of error of optical fractionator population size estimates: a computer simulation comparing three estimators. *J Microsc* 1998;192:163–71. [PubMed: 9853373]
- Gomez-Isla T, Hollister R, West H, Mui S, Growdon JH, Petersen RC, Parisi JE, Hyman BT. Neuronal loss correlates with but exceeds neurofibrillary tangles in Alzheimer's disease. *Ann Neurol* 1997;41:17–24. [PubMed: 9005861]
- Gundersen HJ. Stereology of arbitrary particles. A review of unbiased number and size estimators and the presentation of some new ones, in memory of William R. Thompson *J Microsc* 1986;143 (Pt 1): 3–45.
- Gundersen HJ, Bendtsen TF, Korbo L, Marcussen N, Moller A, Nielsen K, Nyengaard JR, Pakkenberg B, Sorensen FB, Vesterby A, et al. Some new, simple and efficient stereological methods and their use in pathological research and diagnosis. *Apmis* 1988;96:379–94. [PubMed: 3288247]
- Guo Y, Saloupis P, Shaw SJ, Rickman DW. Engraftment of adult neural progenitor cells transplanted to rat retina injured by transient ischemia. *Invest Ophthalmol Vis Sci* 2003;44:3194–201. [PubMed: 12824271]
- Hanninen VA, Pantcheva MB, Freeman EE, Poulin NR, Grosskreutz CL. Activation of caspase 9 in a rat model of experimental glaucoma. *Curr Eye Res* 2002;25:389–95. [PubMed: 12789547]
- Hou B, You SW, Wu MM, Kuang F, Liu HL, Jiao XY, Ju G. Neuroprotective effect of inosine on axotomized retinal ganglion cells in adult rats. *Invest Ophthalmol Vis Sci* 2004;45:662–7. [PubMed: 14744912]
- Huang W, Dobberfuhr A, Filippopoulos T, Ingelsson M, Fileta JB, Poulin NR, Grosskreutz CL. Transcriptional up-regulation and activation of initiating caspases in experimental glaucoma. *Am J Pathol* 2005a;167:673–81. [PubMed: 16127148]
- Huang W, Fileta JB, Dobberfuhr A, Filippopolous T, Guo Y, Kwon G, Grosskreutz CL. Calcineurin cleavage is triggered by elevated intraocular pressure, and calcineurin inhibition blocks retinal ganglion cell death in experimental glaucoma. *Proc Natl Acad Sci U S A* 2005b;102:12242–7. [PubMed: 16103353]
- Hyman BT, Gomez-Isla T, Irizarry MC. Stereology: a practical primer for neuropathology. *J Neuropathol Exp Neurol* 1998;57:305–10. [PubMed: 9600222]
- Isenmann S, Wahl C, Krajewski S, Reed JC, Bahr M. Up-regulation of Bax protein in degenerating retinal ganglion cells precedes apoptotic cell death after optic nerve lesion in the rat. *Eur J Neurosci* 1997;9:1763–72. [PubMed: 9283831]
- Larsen JO. Stereology of nerve cross sections. *J Neurosci Methods* 1998;85:107–18. [PubMed: 9874147]
- Levkovitch-Verbin H, Quigley HA, Martin KR, Valenta D, Baumrind LA, Pease ME. Translimbal laser photocoagulation to the trabecular meshwork as a model of glaucoma in rats. *Invest Ophthalmol Vis Sci* 2002;43:402–10. [PubMed: 11818384]
- Linden R, Perry VH. Massive retinotectal projection in rats. *Brain Res* 1983;272:145–9. [PubMed: 6616190]
- Maeda K, Sawada A, Matsubara M, Nakai Y, Hara A, Yamamoto T. A novel neuroprotectant against retinal ganglion cell damage in a glaucoma model and an optic nerve crush model in the rat. *Invest Ophthalmol Vis Sci* 2004;45:851–6. [PubMed: 14985301]
- McKinnon SJ. Glaucoma: ocular Alzheimer's disease? *Front Biosci* 2003;8:s1140–56. [PubMed: 12957857]
- Moore CG, Milne ST, Morrison JC. Noninvasive measurement of rat intraocular pressure with the Tonopen. *Invest Ophthalmol Vis Sci* 1993;34:363–9. [PubMed: 8440590]
- Morrison JC, Moore CG, Deppmeier LM, Gold BG, Meshul CK, Johnson EC. A rat model of chronic pressure-induced optic nerve damage. *Exp Eye Res* 1997;64:85–96. [PubMed: 9093024]
- Park KH, Cozier F, Ong OC, Caprioli J. Induction of heat shock protein 72 protects retinal ganglion cells in a rat glaucoma model. *Invest Ophthalmol Vis Sci* 2001;42:1522–30. [PubMed: 11381056]
- Quigley HA. Neuronal death in glaucoma. *Prog Retin Eye Res* 1999;18:39–57. [PubMed: 9920498]
- Ronn LC, Ralets I, Hartz BP, Bech M, Berezin A, Berezin V, Moller A, Bock E. A simple procedure for quantification of neurite outgrowth based on stereological principles. *J Neurosci Methods* 2000;100:25–32. [PubMed: 11040363]

- Schlamp CL, Johnson EC, Li Y, Morrison JC, Nickells RW. Changes in Thy1 gene expression associated with damaged retinal ganglion cells. *Mol Vis* 2001;7:192–201. [PubMed: 11509915]
- Schmitz C, Hof PR. Design-based stereology in neuroscience. *Neuroscience* 2005;130:813–31. [PubMed: 15652981]
- Selles-Navarro I, Villegas-Perez MP, Salvador-Silva M, Ruiz-Gomez JM, Vidal-Sanz M. Retinal ganglion cell death after different transient periods of pressure-induced ischemia and survival intervals. A quantitative in vivo study. *Invest Ophthalmol Vis Sci* 1996;37:2002–14. [PubMed: 8814140]
- Tandrup T. Unbiased estimates of number and size of rat dorsal root ganglion cells in studies of structure and cell survival. *J Neurocytol* 2004;33:173–92. [PubMed: 15322376]
- West MJ, Slomianka L, Gundersen HJ. Unbiased stereological estimation of the total number of neurons in the subdivisions of the rat hippocampus using the optical fractionator. *Anat Rec* 1991;231:482–97. [PubMed: 1793176]
- West MJ, Kawas CH, Stewart WF, Rudow GL, Troncoso JC. Hippocampal neurons in pre-clinical Alzheimer's disease. *Neurobiol Aging* 2004;25:1205–12. [PubMed: 15312966]
- Williams RW, Strom RC, Goldowitz D. Natural variation in neuron number in mice is linked to a major quantitative trait locus on Chr 11. *J Neurosci* 1998;18:138–46. [PubMed: 9412494]

**A.****B.****Figure 1.**

Uniform random sampling of a tissue section (A) and a retinal cross section (B). The area around the retina is delineated (black line/arrows) with the CAST system and random systematic samples, locations marked by + symbols (inset), are taken throughout the entire delineated area.

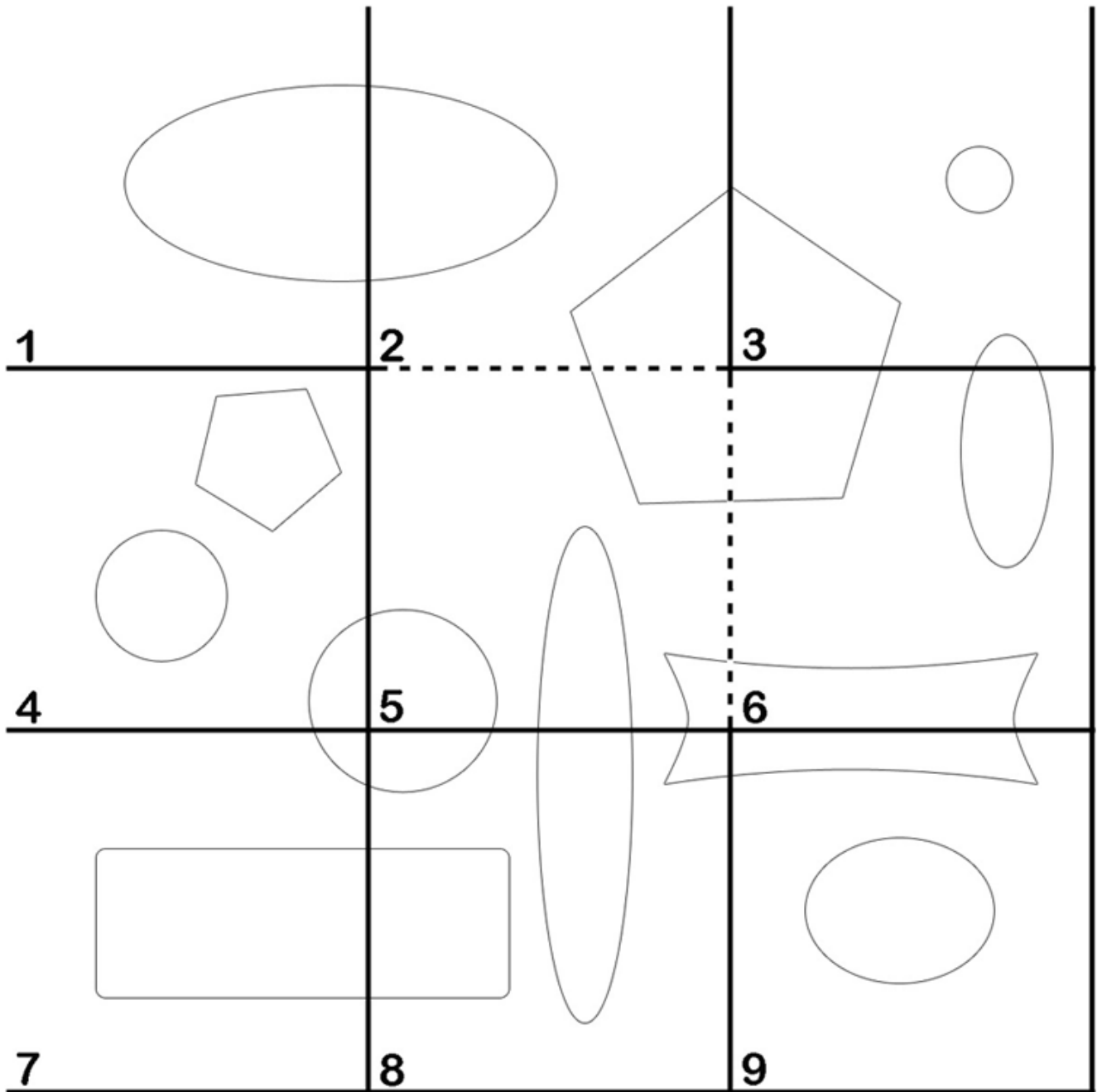


**Figure 2.**

Application of the counting frame. By dividing a planar region into consecutively numbered frames, profiles can be counted and an accurate estimate obtained from a sample fraction.

Frame 2 demonstrates the counting rules for an individual frame: All profiles within the frame are counted as long as they do not touch the exclusion line (solid line) that extends to infinity. All profiles within the frame, partly or completely, in addition to those touching the inclusion line (dashed line) are counted. To estimate the total number of profiles by counting one third of the population, every third frame would be counted after randomly starting with any one of the first three frames. This would result in the assessment of frames: 1, 4, and 7 (counting 5

profiles), 2, 5, and 6 (counting 3 profiles), and 3, 6, and 9 (counting 3 profiles). The mean of these three counts is 3.66, the correct number of one third of the population.

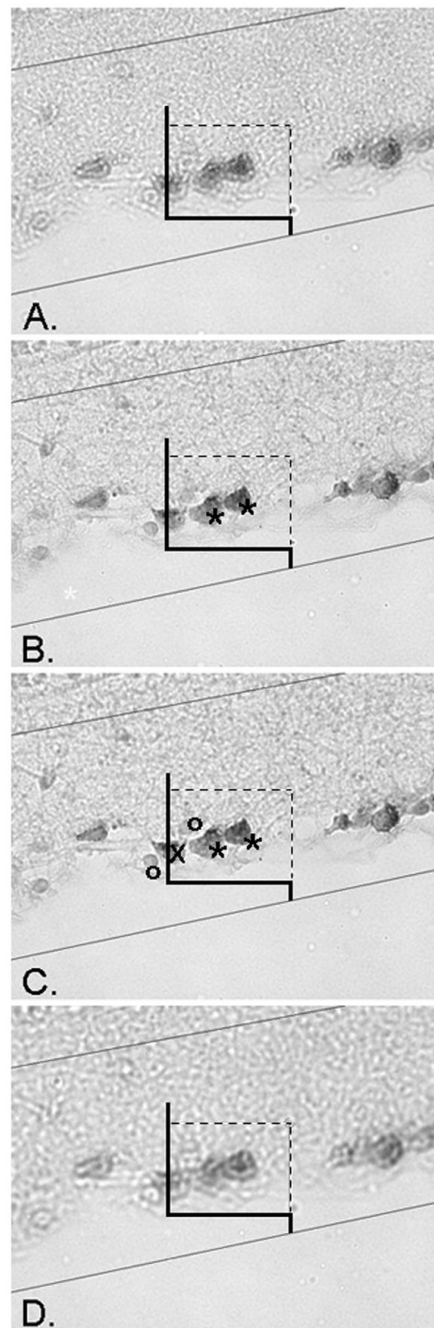


**Figure 3.**

Application of the optical dissector. The counting frame is applied in a randomly sampled area of the retina, then systematically moved and sampled throughout the entire section (Figure 1). At each sampled position the focal plane of the dissector is moved through the thickness of the section and RGC profiles counted. The upper and lower planes of the section serve as exclusion areas, where profiles are not counted. Micrograph A displays the uppermost plane of the section, when an object first comes into focus. It is important to note that any profiles in focus at this upper plane are not counted. The focal plane is moved through the section from (A) to (D) and all RGCs that come into focus within the frame, obeying the counting frame rules (Figure 2), are counted. In micrograph B, two RGCs are marked with asterisks and counted



because they are within the frame, but not in contact with the two forbidden dashed exclusion lines or their extensions. Micrograph C displays the same two counted RGCs further in the focal plane of the section. Note two non-RGC cells marked by circles that are not counted, in addition to the RGCs marked by an X intersecting with the dashed forbidden exclusionary line, and therefore not counted. The plane is focused through the section until the end (D). In this 4 level example, the height of the dissector,  $h$ , from level (A) to level (D) is 11  $\mu\text{m}$ .

**Table 1**

Sampling Intensity Affect on RGC Profile Counts

Trial #	N <sup>th</sup> Section Counted	Total Sections Counted	$\Sigma Q$	CE	Total RGC Estimate
1	6	41	540	0.04	83,327
2	12	22	322	0.06	85,609
3	18	15	215	0.07	83,707
4	24	11	157	0.08	83,353
5	30	8	104	0.10	75,920
6	36	8	119	0.09	86,870
7	42	7	91	0.10	75,920
	Mean				82,101
	STD				4,418
	CV				0.05

**Table 2**

Stereological Estimate of Total RGC Number in a Brown Norway Rat Retina

Animal #	RGC Count ( $\Sigma Q$ )	Coefficient of Error (CE)	Total RGC Estimate
1	262	0.06	80,706
2	239	0.06	88,918
3	210	0.07	90,400
4	221	0.07	86,279
5	202	0.07	80,327
6	229	0.06	89,864
7	225	0.07	79,748
8	239	0.06	93,422
9	210	0.07	84,752
10	181	0.07	88,400
Mean	221.8	0.066	86,282
STD	22.6	0.005	4,759
CV			0.06

**Table 3**

Loss of RGC from Experimental Glaucoma

Animal	Control Eye	CE	Experimental	CE
1	78,373	0.072	51,396	0.067
2	90,950	0.070	63,029	0.058
3	84,026	0.065	57,600	0.056
4	80,300	0.070	53,005	0.063
5	93,600	0.065	62,037	0.056
6	87,350	0.074	58,764	0.062
7	78,000	0.068	51,100	0.065
8	86,259	0.067	57,600	0.059
Mean	84,862	0.069	56,837	0.061
STD	5,753	0.003	4,272	0.004
CV	0.07		0.08	